Spectroscopic Effects of Polarity and Hydration in the Distal Heme Pocket of Deoxymyoglobin†

J. F. Christian, M. Unno,‡ J. T. Sage, and P. M. Champion*

Department of Physics and Center for Interdisciplinary Research on Complex Systems, 111 Dana Research Center, Northeastern University, Boston, Massachusetts 02115

E. Chien§ and S. G. Sligar

Departments of Biochemistry and Chemistry, University of Illinois, Urbana, Illinois 61801

Received April 30, 1997; Revised Manuscript Received June 30, 1997⊗

ABSTRACT: Distal pocket mutations at the E7 position (His64) of sperm whale deoxymyoglobin (deoxyMb) are used as a probe of distal pocket polarity and hydration. Changes of two key spectroscopic markers, the Fe−His(F8) stretch in the resonance Raman spectrum and the position of band III in the absorption spectrum, are monitored as the His64Tyr, His64Phe, His64Leu, and His64Gly mutations alter the distal heme pocket environment. The Fe−His vibration for the Phe, Leu, and Gly mutants is shifted to a lower frequency by 1−2 cm^{-1} relative to the Tyr mutant, wild type (WT), and native deoxyMb. Band III shifts to the red by ∼4 nm (∼70 cm^{-1}) relative to WT and native deoxyMb for all the His64 mutants examined in this work. We correlate the small shift in the Fe−His frequency to the local electrostatic environment directly above the heme iron, affected by the presence of a localized water molecule in the heme pocket that is hydrogen-bonded to the E7 residue. The position of band III is roughly correlated to the displacement of the iron from the heme plane; however, the relatively large scatter in this correlation, as well as its dependence on distal pocket mutations, suggests that the heme pocket environment, particularly the E7 residue, also affects the energy of this transition.

Myoglobin (Mb)[1] is a small heme-containing protein that functions as a reversible oxygen carrier. It is extensively studied as a model for exploring the relationship between protein structure, dynamics, and function (Sage & Champion, 1996). Optical spectroscopies, such as resonance Raman scattering, are often used to characterize myoglobin and other heme proteins because the active site contains the strongly absorbing heme chromophore. An important spectroscopic marker in the resonance Raman scattering of deoxyhemoglobin (deoxyHb) and deoxyMb is the Fe−His(F8) stretching frequency. The Fe−His(F8) bond links the heme active site to the protein matrix, and the stretching frequency of this bond, in deoxyHb, has been directly correlated to the allosteric conformations of the protein, and thus to the ligand binding affinity (Matsukawa et al., 1985; Rousseau & Friedman, 1988). In deoxyMb, the stretching frequency of this Fe−His(F8) bond (Fe−His93) has also been shown to be sensitive to the protein structure and relaxation dynamics (Rousseau & Friedman, 1988; Sage et al., 1995; Schulte et al., 1995). Another important spectroscopic marker is the band III transition in the absorption spectrum of ferrous high-spin heme proteins. Band III has been assigned to the $a_{2u} \rightarrow d_\pi$ transition (Eaton et al., 1978), where an electron is promoted from the porphyrin π orbital to the heme iron d_π orbital. It is a convenient structure-sensitive band (Iizuka et al., 1974; Campbell et al., 1987; Šrajer & Champion, 1991) whose position can be associated with a displacement of the iron out of the heme plane and the tilting of the Fe−His bond (Šrajer & Champion, 1991; Kiger et al., 1995; Chavez et al., 1990; Sassaroli & Rousseau, 1987; Jackson et al., 1994). These spectroscopic markers are traditionally used as probes to infer structural information about the proximal side of the heme pocket. The influence of the distal pocket environment on these markers, however, is less well understood.

The protein backbone envelops the heme active site and provides an environment that mediates its reactivity. Figure 1 shows the environment of the heme active site in wild-type (WT) sperm whale (SW) deoxyMb from the X-ray crystal structure (Quillin et al., 1993).[2] As seen in Figure 1, WT deoxyMb contains a localized water molecule in the distal heme pocket that is hydrogen-bonded to the E7 residue (His64) (Springer et al., 1989); in other words, the distal pocket is polar and hydrated. Native and WT deoxyMb have identical residues in the heme pocket, they only differ because the WT protein contains an accidental Asp122Asn mutation and a methionine initiator (Springer & Sligar, 1987). Mutating the His64 residue probes the effect of polarity and hydration in the distal pocket on the heme active site. Replacing His64 with Leu makes the distal heme pocket apolar, since the X-ray crystal structure shows the absence of distal pocket water in the deoxy state of this mutant

† This work was supported by NIH Grant DK-35090 (P.M.C.), NSF Grant 94-05979 (P.M.C.), and NIH Grants GM31756 (S.G.S.) and GM33775 (S.G.S.).

* To whom correspondence should be addressed.

‡ Present address: Institute for Chemical Reaction Science, Tohoku University, Sendai 980, Japan.

§ Present address: Chemistry Department, University of California, Davis, CA 95616.

⊗ Abstract published in *Advance ACS Abstracts,* August 15, 1997.

[1] Abbreviations: Mb, myoglobin; Hb, hemoglobin; deoxyMb and Mb(Fe^{2+}), deoxymyoglobin; deoxyHb, deoxyhemoglobin; Fe−His, iron−histidine; WT, wild type; SW, sperm whale; Mb(Fe^{3+}), metmyoglobin; ν_{Fe-His}, stretching frequency of Fe−His bond; NMR, nuclear magnetic resonance.

[2] Figure 1 was rendered with RasMol; Roger Sayle, Glaxo Research & Development; Greenford, Middlesex, U.K.

S0006-2960(97)01007-6 CCC: $14.00

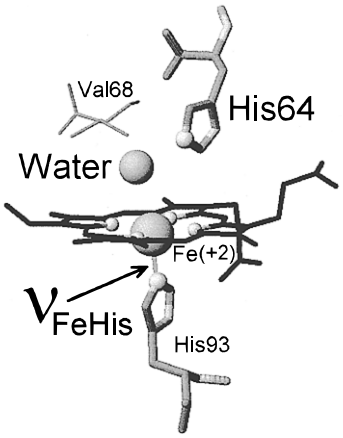

FIGURE 1: Heme environment of wild-type sperm whale deoxymyoglobin (Quillin et al., 1993). The figure illustrates the following features of the heme pocket environment: the oxygen atom of the hydrogen-bonded water molecule, the Fe−His bond (with a stretching frequency denoted by ν_{Fe-His}), and the distal histidine (His64).[2]

(Quillin et al., 1993). The "core size" marker bands in the resonance Raman spectrum show that the His64Leu mutation also prevents water from coordinating to the heme iron in the ferric oxidation state, Fe^{3+} (unpublished results), consistent with previous work (Ikeda-Saito et al., 1992; Quillin et al., 1993) that demonstrated the absence of this coordinated water. Replacing His64 with the smaller, apolar Gly residue increases the space in the distal pocket, and the X-ray crystal structure reveals the presence of a water molecule in the distal heme pocket of the deoxy form. This water molecule is further from the heme iron, 4.5 Å, than the localized water molecule that is hydrogen-bonded to the distal histidine in WT deoxyMb and found 3.9 Å from the heme iron (Quillin et al., 1993). In the His64Gly mutant, the water molecule does not appear to be hydrogen-bonded to any residue in the heme pocket, and its occupancy number is 0.38 (compared to 0.84 for the pocket water molecule in WT deoxyMb). The polar Tyr residue is large enough for its hydroxyl group, OH, to coordinate to the heme iron in met-His64Tyr Mb(Fe^{3+}) (Egeberg et al., 1990; Pin et al., 1994; Hargrove et al., 1994), making the hydration of the distal pocket in the deoxy state unlikely. In the proposed structure (Pin et al., 1994), the protruding OH group in the Tyr mutant appears to effectively replace the localized water molecule that is hydrogen-bonded to the distal His in native and WT deoxyMb. Phenylalanine (Phe) is essentially a Tyr residue without the polar hydroxyl group (OH), and like the His64Leu mutant, the His64Phe mutation prevents water from entering the heme pocket even in the ferric oxidation state, Mb(Fe^{3+}) (Morikis et al., 1990). In other words, if the heme environment excludes water from the distal pocket in the ferric form, where the water would like to chemically bond to the heme iron, then apparently water is also excluded from the distal pocket in the ferrous form (Quillin et al., 1993). Overall, the His64Phe mutation produces an anhydrous and apolar distal pocket.

Previous work has examined the effect of the distal pocket environment in Mb on ligand binding affinity (Springer et al., 1994), as well as on the contact shifts in the NMR spectrum (La Mar et al., 1994). In this work, we present resonance Raman experiments on mutant Mbs, whose His64 residue has been replaced by Tyr, Phe, Leu, and Gly, and we examine the effect of the distal pocket environment, polarity, and hydration, on the Fe−His stretching frequency. We also investigate the effect of these mutations on the position of band III in the absorption spectrum.

MATERIALS AND METHODS

Sample Preparation. WT sperm whale myoglobin was purchased from Sigma Chemical Co. (M-7527, lot 85H8916). Previous references (Springer et al., 1989; Springer & Sligar, 1987; Egeberg et al., 1990) describe the preparation of the site-directed mutant samples, which were stored in liquid N_2. The initial buffer in all samples was replaced with 0.1 M borate at pH 8, and the samples were concentrated with Amicon concentrators (Amicon Inc.). All samples were filtered through a 0.2 μm membrane to remove any particles or microbes. The protein concentration was 0.4 mM, which was prepared by diluting a concentrated protein solution into a 0.1 M borate buffer at a pH of 8. The relatively high protein concentration helps resolve the low-frequency Raman modes of the protein by decreasing the relative contribution from the solvent.

To reduce the sample, approximately 2 μL of a ~340 mM dithionite ($Na_2S_2O_4$) solution (in buffer) was added to 20 μL of sample, in a 3 × 3 × 48 mm quartz cuvette (NSG Precision Cells), after deoxygenating with a flow of Ar for approximately 10 min. The punctured septum was sealed with vacuum grease, and the samples were centrifuged at ~25000*g*, in the cuvette, for 10 min to "spin down" any particles. His64Gly was kept at 4 °C until its measurement at room temperature, because we found that this particular deoxyMb sample is unstable (Morikis, 1990), as evidenced by a shoulder in the absorption spectra at ~640 nm, which slowly develops over time. After each Raman measurement, the absorption spectrum was measured (using a Hitachi U-3410 spectrophotometer) to verify the integrity of the sample.

Resonance Raman Setup. Measurement of a resonance Raman spectrum starts with the collection of light that is scattered at 90° from an incident 441.6 nm excitation beam of a HeCd laser (Omnichrome Inc.), whose power is ~3 mW at the sample. An interferometric notch filter (Kaiser Instruments) rejects the laser light before the image is focused onto the slit of a single grating monochromator (Spex Industries 1870B). This prevents the contamination of the low-frequency region of the spectra by the small aberrations in the image of the intense Rayleigh light. It also introduces a slight distortion, or attenuation, of the relative intensities in the low-frequency region of the spectrum, <150 cm^{-1}. In this work, the spectra are not corrected for this attenuation at low frequencies because it is a negligible factor in the region of interest, above 200 cm^{-1}, and it is the same for all the samples. The 100 μm slit width employed in these measurements corresponds to an instrumental resolution of ~3 cm^{-1}, which describes our ability to distinguish adjacent peaks with a 2400 groove/mm grating in the monochromator. A liquid nitrogen cooled charge-coupled device (Princeton Instruments), interfaced to a personal computer, detects and records the frequency-resolved intensity of the scattered light. Spikes in the spectrum due to cosmic radiation are removed by applying a derivative filter subroutine in the commercial data acquisition software. The absolute frequencies relative to the excitation, i.e. the Raman shifts, are calibrated using fenchone as a standard, and we expect an approximately 2 cm^{-1} accuracy in this calibration. Relative frequency shifts

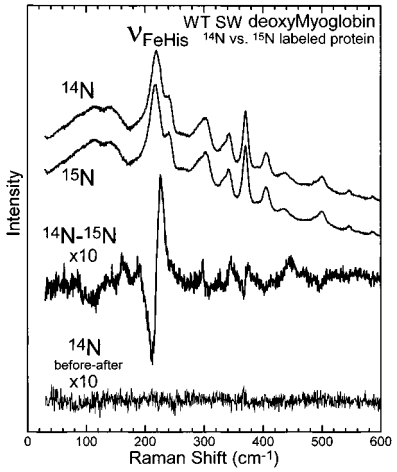

FIGURE 2: Shift induced by labeling the protein of wild-type sperm whale deoxyMb, but not the heme, with ^{15}N, confirming the Fe−His stretching mode assignment for this peak (Argade et al., 1984; Wells et al., 1991). For the Raman experiments, we "sandwich" the measurements of interest between the measurement of "normal" deoxyMb (^{14}N). The difference between the "before" and "after" spectra of the "normal" deoxyMb verifies the integrity of the Raman shifts. These data are acquired under the following conditions: ~3 mW of 442 nm excitation light at the sample, ~0.4 mM protein concentration in a 0.1 M borate buffer at pH 8.

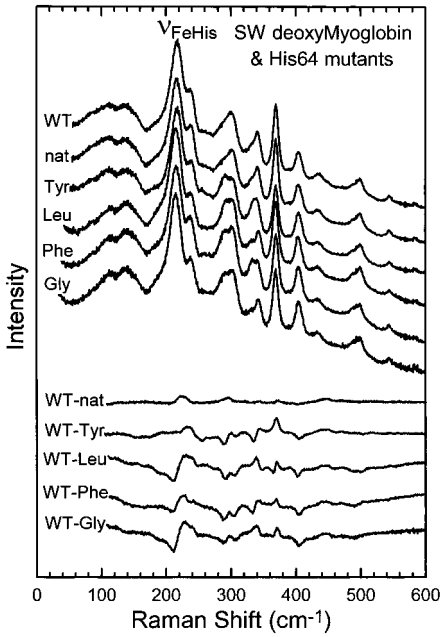

FIGURE 3: Raman spectra of SW deoxyMb, various His64 mutants, and the difference spectra (×1) with respect to WT deoxyMb. The experimental conditions are the same as those in Figure 2.

in the peaks of different samples, however, can be determined with much greater accuracy, ±0.2 cm^{-1}. A polarization scrambler is placed at the entrance of the monochromator.

Samples are prepared sequentially, and run back-to-back in a given set of Raman measurements. The first and last spectrum of the set measures the same sample, and the difference between the first and last spectrum verifies the integrity of the observed shifts. To exemplify the integrity of the relative shifts in a set of measurements, Figure 2 shows the difference between isotopically labeled and unlabeled WT deoxyMb, where the protein is labeled with ^{15}N but the porphyrin of the heme contains natural ^{14}N (Springer & Sligar, 1987; Wells et al., 1991). This measurement faithfully reproduces the observations and assignment of previous studies (Kitagawa et al., 1979; Argade et al., 1984; Wells et al., 1991), demonstrating the Fe−His stretching at ~220 cm^{-1}. Recently, the peak at ~241 cm^{-1} has been assigned to ν_9 (Hu et al., 1996), which is an in-plane porphyrin stretching mode with A_{1g} symmetry (Abe et al., 1978; Li et al., 1990).

We evaluate the difference spectra of the mutation-induced effects, to check for recognizable artifacts, such as the presence of peaks due to quartz or dithionite. These difference spectra, however, are difficult to quantitatively interpret for the following reason: unlike the difference spectrum shown in Figure 2, which compares isotopically labeled samples, the mutations introduce subtle changes in the relative amplitudes and apparent widths of the peaks, as well as shifts in the vibrational frequencies. In Figure 3, distinct shifts in the Fe−His stretching region can be discerned for the Leu, Phe, and Gly mutants; however, the magnitudes of the shifts are difficult to quantify using standard Raman difference algorithms. Therefore, under Results, the Raman spectra are fitted to Lorentzian peaks using commercially available software (Origin, version 3.78, Microcal Software, Inc.).

The entire Raman spectrum was fitted, including the tail produced by Rayleigh scattering and higher frequency Raman modes. Uncertainties for the parameter values recovered in the curve-fitting analysis of both the Raman and absorption spectra, at the 95% confidence level, are consistently smaller than the standard deviation from multiple determinations. Error bars presented in this work represent the deviation from independent determinations of three or more sets of spectra, which we measured within a period of approximately 1 month. Although it has been suggested that the Fe−His peak in deoxyMb consists of discrete conformational substates at low temperature (Gilch et al., 1995), we fit the Fe−His mode with a single Lorentzian at room temperature to reduce the degrees of freedom and to improve the uniqueness of the fit. Therefore, the fits merely quantify the mutation-induced changes in the spectra and are not intended to represent an unambiguous decomposition or assignment of the vibrational structure in the spectra. We also use Lorentzian functions to fit the band III region of the absorption spectra. Fitting the data with Gaussian functions did not improve, or significantly affect, the quality of the fit. However, for a more detailed model of the band III line shapes see Cupane et al. (1988), Cordone et al. (1990), and Šrajer and Champion (1991). In fitting the absorption spectra, we construct the base line from the tail of an absorption band to the blue, and an absorption band in the IR, on a constant offset.

RESULTS

Figure 4 shows the absorption spectra of SW deoxyMb and the His64 mutants in the Q-band and band III regions. As seen in the figure, the absorbance spectra of the native and WT proteins are almost indistinguishable. The Q-band of the Tyr mutant appears to be red-shifted relative to the native and WT samples. This shift is consistent with the previously observed 4 nm shift, from 554 nm in WT to 558 nm in the Tyr mutant (Egeberg et al., 1990). Qualitatively, the shape of the Q-band in native, WT, and the Tyr mutant appears "sharper" than that in the Phe, Leu, and Gly mutants. These spectral changes, however, are difficult to meaningfully quantify because our simple peak-fitting analysis is ambiguous when it is applied to the complicated structure in the Q-band region.

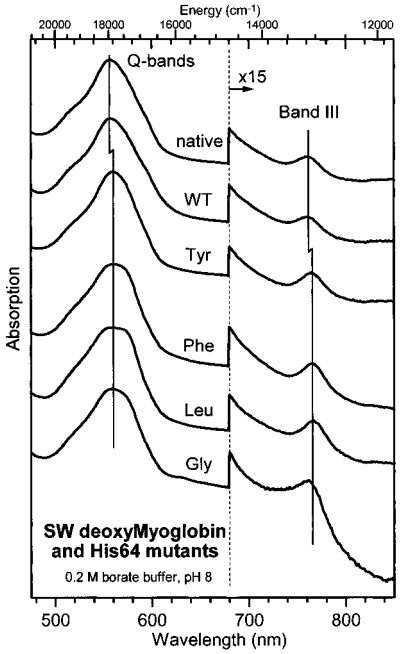

FIGURE 4: These absorption spectra of sperm whale deoxyMb and His64 mutants show the effect of the mutation on the Q-band and band III transitions. The shape of the Q-band in the WT, native, and Tyr samples (forms with a polar distal pocket) appears "sharper" than in the Phe, Leu, and Gly samples (mutants with an apolar heme environment). Band III of the Tyr mutant, however, is red-shifted, relative to its position in the WT and native proteins, along with the Phe and Leu mutants. Some "distortion" in band III of the Gly mutant is a reproducible feature of our sample, which is less stable in the ferrous deoxy state. This distortion is NOT correlated to a known product, met or breakdown, that produces a shoulder in the Q-band region at ~640 nm. Note that all intensities are arbitrarily scaled to equalize the height in the Q-band region.

Figure 4 also shows that the position of band III in the Tyr, Phe, and Leu mutants is red-shifted relative to its position in the native and WT samples. It should be noted that both the Q-band and band III of the Tyr mutant are red-shifted by ~4 nm, while the position of the Soret band, at 433 nm, is indistinguishable from the WT protein (Egeberg et al., 1990). The mutations hardly affect the peak position of the Soret band, which is at 433 nm for all the samples (data not shown), in agreement with previously reported values for WT, native, and the Tyr mutant deoxyMb (Egeberg et al., 1990). However, the mutations do introduce some small and subtle changes in the shape of the Soret band. Curiously, band III in the Gly mutant appears to be distorted and may be composed of multiple components. This distortion is a reproducible feature of our sample, which is less stable in the ferrous deoxy state, Mb(Fe^{2+}), and its presence is not directly linked to the appearance of a shoulder in the Q-band region at ~640 nm (a breakdown or oxidization product).

Table 1 lists the positions and widths of band III for the samples recovered from the fit of the absorption spectra versus energy. Analysis of band III for the Gly mutant requires a minimum of two peaks to give a reasonable fit to the data, i.e., improving χ^2 by a factor of 3. We are not certain about the origin or assignment of this structure. The position of band III for native and WT deoxyMb, at 762 nm, is consistent with previous work (Iizuka et al., 1974; Cupane et al., 1988; Cordone et al., 1990; Šrajer & Champion, 1991; Kiger et al., 1995). Furthermore, the red-shifted position of band III, at ~768 nm, for the Leu and Phe mutants is similar to that seen for other heme proteins with an apolar distal pocket (Kiger et al., 1995; Gilles-Gonzalez et al., 1994). For example, *B. japonicum* FixL [(E7)Phe], *Aplysia* Mb [(E7)Val], and monomeric *Glycera* Hb [(E7)Leu] all have band III maxima near 770 nm.

Table 1: Band III Position and Width in SW DeoxyMb and His64 Mutants[a]

SW Mb sample	band III position ± σ		width ± σ	
	cm^{-1}	nm	cm^{-1}	nm[b]
native	13121 ± 3	762.1 ± 0.3	583 ± 28	34 ± ~3
WT	13117 ± 4	762.4 ± 0.4	583 ± 7	34 ± ~1
His64Tyr	13058 ± 4	765.8 ± 0.4	552 ± 25	32 ± ~3
His64Phe	13036 ± 3	767.1 ± 0.3	544 ± 27	32 ± ~3
His64Leu	13018 ± 4	768.2 ± 0.4	558 ± 23	33 ± ~3
His64Gly	~13075	~765	~688	~40
	{~13580	~736	~1360	~74}[c]

[a] Frequencies and widths are obtained from the fit of the absorption vs energy, using Lorentzian line shapes. Base lines are constructed from the tail of an absorption band to the blue and an absorption band in the IR on a constant offset. The uncertainties, σ, are the standard deviations calculated from three, or more, independent determinations. [b] The translation of the uncertainties in the peak width to the units of nanometers is given as an approximation of the peak characteristics in the measured spectrum. [c] The analysis of band III in the Gly mutant requires a minimum of two peaks to give a reasonable fit to the data, with a factor of 3 improvement in χ^2. We are not certain about the origin and assignment of this structure; however, it is a reproducible feature of our sample, which is less stable in the ferrous deoxy state, and it is not directly correlated to the familiar breakdown, or met, product.

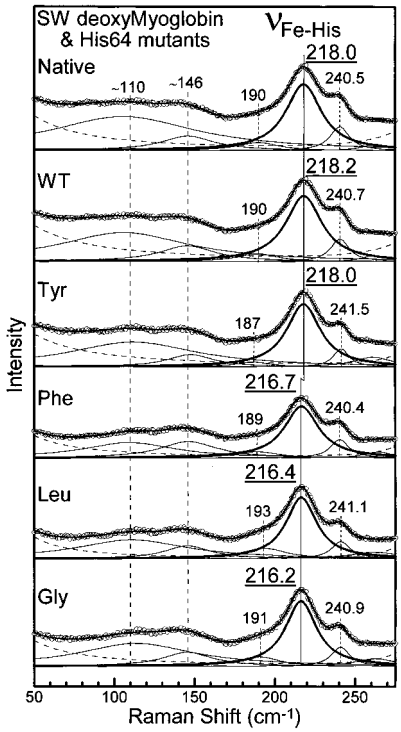

FIGURE 5: Effect of distal pocket mutations on the Fe−His and other low-frequency modes in a typical resonance Raman measurement of sperm whale deoxyMb and the His64 mutants. The Fe−His frequency of the Phe, Leu, and Gly mutants is lower than that of WT, native, and the Tyr mutant. The experimental conditions are the same as those in Figure 2. The intensities are arbitrarily scaled, and the peaks are fitted using Lorentzian functions on a constant base line. The fits merely quantify the mutation-induced changes in the spectra and are not intended to represent an unambiguous decomposition or assignment of the vibrational modes in the spectra.

Figure 5 shows the effect of distal pocket mutations on the Fe−His and other low-frequency vibrations in a typical

Table 2: Position and Width for the Fe−His Stretching Mode in SW DeoxyMb and His64 Mutants from the Resonance Raman Spectra[a]

SW Mb sample	Fe−His frequency ± σ (cm^{-1})	width ± σ (cm^{-1})
native	217.8 ± 0.15	26.4 ± 0.6
WT	218.2 ± 0.06	26.9 ± 0.5
His64Tyr	218.1 ± 0.06	25.2 ± 0.4
His64Phe	216.8 ± 0.15	25.3 ± 0.7
His64Leu	216.5 ± 0.12	23.4 ± 1.0
His64Gly	216.3 ± 0.06	24.5 ± 0.8

[a] Frequencies and widths are obtained from the average of three experiments with a commercial fitting program using Lorentzian line shapes. The uncertainties, σ, are the standard deviations calculated from three independent determinations (measurements and ensuing analysis). The fitting quantifies the mutation-induced changes in the spectra and is not intended to represent an unambiguous assignment or decomposition of the vibrational structure in the spectra. The conditions for all measurements are the same as those given in Figure 2.

resonance Raman measurement of SW deoxyMb and the His64 mutants. Experimental conditions are the same as those in Figure 2. The Fe−His frequency of the Phe, Leu, and Gly mutants is lower than that of WT, native, and the Tyr mutant. Also, the intensity of the low-frequency structure at ∼110 cm^{-1} in the native, WT, and Tyr mutants is larger, relative to the other peaks, than that in the Phe, Leu, and Gly mutants. The 241 cm^{-1} mode of Tyr, Leu, and Gly is slightly upshifted, by ∼0.5 cm^{-1}, relative to the other samples. In Figure 5, we incorporate the tails of the peaks that are outside of the plot region into the base line.

Although there are other subtle differences in the spectra, we will focus primarily on the Fe−His mode because it exhibits the largest perturbation induced by the mutation, and because the assignment of this mode is well established. The frequency of the Fe−His stretch in the Tyr mutant, relative to WT, is consistent with previous work (Egeberg et al., 1990), and the intensity of the Fe−His mode for the Phe and Gly mutants, relative to the 241 cm^{-1} mode, is also in agreement with previous work (Morikis, 1990; Morikis et al., 1989).

Table 2 lists the positions and widths for the Fe−His stretching mode in SW deoxyMb and the His64 mutants. The small difference between the Fe−His frequency of native and WT is not certain; i.e., they are within the experimental error for 95% confidence limits. On the other hand, the difference between the Fe−His frequency of native, WT, and the Tyr mutants, at ∼218 cm^{-1}, and the Phe, Leu, and Gly mutants, at ∼216.5 cm^{-1}, is well outside the experimental error. The widths of the Fe−His mode in the native and WT samples may be slightly larger than those in the His64 mutants, but the relatively large uncertainty precludes any definite correlations.

DISCUSSION

Effect of the Distal Pocket Environment on the Fe−His Stretching Frequency. Figure 5 and Table 2 clearly demonstrate that the distal pocket environment perturbs the Fe−His stretching frequency, producing shifts of approximately 1−2 cm^{-1}. Specifically, we suggest that a decreased polarity in the local environment above the heme iron in the distal pocket, which occurs in the Phe, Leu, and Gly mutants, decreases the Fe−His frequency. Evidently, the presence of a localized water molecule that is hydrogen bonded to the distal histidine, or the polar OH group of the Tyr mutant, produces an electrostatic perturbation in the iron orbitals and we propose that this perturbation increases the nominal Fe−His stretching frequency. The direction of this shift suggests a weak interaction between the iron orbitals and the negative electron density of the water molecule or the OH group in the Tyr mutant (probably the lone pair electrons of the oxygen atom). To test this interpretation, we examined the Fe−His stretching frequency of the Leu29Phe mutant, listed in Table 3, which has a dehydrated heme pocket (Carver et al., 1992; Quillin, 1995). As expected, the frequency of the Fe−His stretch in this mutant is approximately 1 cm^{-1} less than that in the WT protein. We speculate that the localized water molecule in WT Mb and the protruding OH group in the Tyr mutant produce a negative electrostatic environment in the distal pocket, which slightly polarizes the iron d-orbitals and increases the trans Fe−His bond strength.[3] In comparing vibrational frequencies, we can infer an increase in the bond stability, or bond energy, because the "width" of the internuclear potential, which determines the vibrational energy level spacing, is often correlated with the "depth" of the internuclear potential. We note that the dependence of the Fe−His stretching frequency on the heme environment, specifically on the polarity introduced by the hydrogen-bonded water, is consistent with the trends observed for the shifts in the NMR spectra of distal pocket mutants by LaMar et al. (1994). Their work demonstrates that the $N_\delta H$ proximal histidine contact shifts are also sensitive to the presence of the localized water molecule in the distal pocket.

We should also note that the observed ∼1−2 cm^{-1} shifts in the Fe−His frequency due to changes in the distal pocket environment are considerably smaller than those correlated to the allosteric conformational change in hemoglobin, which shifts the Fe−His frequency by ∼8 cm^{-1} (Matsukawa et al., 1985; Rousseau & Friedman, 1988; Kiger et al., 1995; Nagai & Kitagawa, 1980). In many cases, the conformation of the protein may be the dominant factor in determining the Fe−His stretching frequency. To compare the results of this work to that of Kiger et al., Table 3 lists the Fe−His stretching frequency, the position of band III, the ligand binding kinetics, and various structural characteristics for the deoxyMb mutants studied in this work. This table shows the upshifted Fe−His stretching frequency at 218 cm^{-1} correlates with the presence of localized water or OH in the distal pocket. It also demonstrates that there is only a "loose" correlation between the ligand binding rate and the Fe−His stretching frequency in SW deoxyMb, unlike hemoglobin where the ligand binding properties, and the Fe−His stretching frequency, are strongly influenced by the allosteric conformation of the protein.

A slight difference in the width of the Fe−His mode for the different mutants, as seen in Table 2, may be caused by different populations of conformational substates (Gilch et al., 1995). Since we cannot uniquely decompose the Fe−His mode into subbands, our observations of the position and width of this mode refer to nominal, or average, values. With proper consideration of the relatively large uncertainty in the peak width, we note that the differences in the Fe−His band width may be weakly correlated to the shift in band III; i.e., the width of the Fe−His peak for native and WT, ∼26.5 cm^{-1}, is slightly larger than that for the mutants, ∼25 cm^{-1}.

[3] In this context, bond strength is equivalent to the force constant or second derivative of the internuclear potential, unlike other usages that equate the bond strength to the bond energy or depth of the internuclear potential.

Table 3: Band III Position, Fe−His Stretching Frequency, and Ligand Binding Kinetics (k_{on}) of CO and O_2 for SW DeoxyMb and His64 Mutants

SW Mb sample	band III (nm)	Fe−His stretch (cm^{-1})	binding rate, k_{on} (μM^{-1} s^{-1})[a]		Fe distance (Å) from heme plane[b] (from N-plane)	Fe−His bond distance[b] (Å)	local pocket water/OH
			CO	O_2			
WT	762	218	0.51	17	0.41 (0.32)	2.24	yes
His64Tyr	766	218	0.50	6.7	−	−	yes
His64Phe	767	217	4.5	75	−	−	no
His64Leu	768	216.5	26	98	0.24 (0.20)	2.29	no
His64Gly	765	216	5.8	140	0.37 (0.27)	2.22	no
Leu29Phe	762	217	0.22	21	0.36 (0.28)	2.32	no

[a] Data are obtained from Springer et al. (1994) and references cited therein. The ligand binding rate, k_{on}, is defined with respect to the chemical equation:

$$\mathrm{Mb} + \mathrm{L} \underset{k_{off}}{\overset{k_{on}}{\rightleftharpoons}} \mathrm{MbL}$$

where L is the O_2 or CO ligand. As can be seen, there does not appear to be a direct correlation between these spectroscopic markers and the ligand binding rate. [b] Structural information is obtained from the following X-ray crystal structures in the Brookhaven protein data base: WT (2MgL), His64Leu (2MgD), His64Gly (1Mob), Leu29Phe (1MoA).

Effect of the Distal Pocket Environment on the Absorption Spectra. Intriguingly, the distal pocket environment also affects the absorption spectra, specifically the position of band III, as shown in Figure 4 and Table 1. All of the His64 mutations examined in this work shift the position of band III toward the red, by ∼70 cm^{-1}, relative to the native and WT proteins. As seen in Table 3, the change in position of band III is not strictly correlated with the change in the Fe−His frequency for the SW deoxyMb samples. Table 3 also shows that the position of band III for the Leu29Phe mutant, which does not have a water molecule in the distal pocket, is very similar to that in WT deoxyMb. Since band III of all His64 mutants in this study is red-shifted, and band III of WT and Leu29Phe is not red-shifted, we are able to conclude that the position of band III is not directly correlated to the hydration of the distal heme pocket (in contrast to the Fe−His frequency). Furthermore, Table 3 supports the observation by Marden et al. (Kligar et al., 1995) that the position of band III is not correlated to the CO binding rate in Mb mutants with an apolar distal pocket.

One remaining explanation for the difference in band III positions is that the presence of His64 blue-shifts the transition, perhaps due to electric fields in the heme pocket. This explanation is supported by recent studies of charge transfer bands in aquo metMb, which have been shown to be sensitive to electrostatic perturbations induced by distal pocket mutations (Varadarajan et al., 1989).

We plot the position of band III versus the iron displacement in Figure 6 because the position of band III is often used as a structural marker (Iizuka et al., 1974) for the displacement of the iron from the heme plane (Campbell et al., 1987; Šrajer & Champion, 1991; Sassaroli & Rousseau, 1987; Jackson et al., 1994). This plot includes band III measurements of the mutants in this study, whose X-ray crystal structures are known, together with a variety of other heme proteins. As illustrated in the figure, a red-shifted band III is roughly correlated to a smaller iron displacement from the heme plane. There is, however, a fair amount of scatter in this correlation. This scatter may be entirely due to the uncertainties in the X-ray crystal structure. If this is true, then Figure 6 shows that the uncertainties are greater than 0.1 Å. An alternative explanation for the scatter in Figure 6 is that another factor, a "distal effect", influences the position of band III, and contributes to the observed scatter. It is also important to note that in this figure, the position of band III is determined from the absorption of protein solutions, whereas the structure is determined from the diffraction of protein crystals.

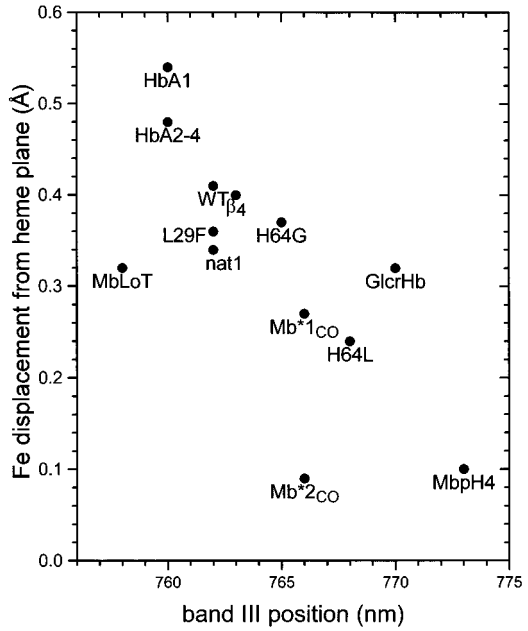

FIGURE 6: Information obtained from the following X-ray crystal structures: wild type (WT:1MgL); native (nat1:1MbD); SW His64Leu (H64L:2MgD); SW His64Gly (H64G:1MoB); SW Leu29Phe (L29F:1MoA); human hemoglobin, HbA, low salt, Cl^- (HbA1:1HbB); human HbA [HbA2−4:(2−4)HhB]; tetramer β chain of human Hb (β_4:1CbL); *G*lycera Hb [GlcrHb:2HbG, monomeric His(E7)Leu]; SW myoglobin pH 4 (MbpH4:1VxA); low-temperature Mb [MbLoT (Schlichting et al., 1994)]; and Mb*1_{CO} and Mb*2_{CO} photoproducts: Mb*1_{CO} (Schlichting et al., 1994); Mb*2_{CO} (Teng et al., 1994)]. Structural values for the tetramers are the average of the subunits, and low-temperature band III positions, including the photoproduct, are an average of the values reported in references (Šrajer & Champion, 1991; Cordone et al., 1990; Nienhaus et al., 1992; Steinbach et al., 1991; Fiamingo & Alben, 1984); Palaniappan & Bocian, 1994; pH 4 sample may be partially unfolded).

Figure 4 shows that the distal pocket mutation also affects the Q-band region of the absorption spectrum. In comparing the Q-bands of the Tyr mutant to WT Mb, specifically the similarity in shape but ∼4 nm red-shift (along with band III, which also shifts ∼4 nm), we can suggest that the perturbation responsible for the red-shifted absorption in the Tyr mutant simply shifts the energy of the a_{2u} orbital, which is common to both the Q-band and band III transitions. Finally, we note that the apolar environment of the Phe, Leu,

and Gly mutants produces additional distortions in the shape of the Q-band region, i.e., an apparent increase in the width. This distortion might be associated with the absence of a localized water molecule (or OH group) in the distal pocket; however, it is considerably smaller in the Leu29Phe mutant (data not shown), which also lacks a localized water molecule (or OH group) in the distal pocket.

CONCLUSION

Mutation-induced shifts in the Fe−His stretching frequency illustrate that the environment of the distal heme pocket can influence the proximal Fe−His bond in SW deoxyMb. The changes observed in the spectroscopic markers are directly linked to properties of the distal heme pocket environment, such as hydration, polarity, or electrostatic effects that are explicitly altered by the His64 mutations. We observe small shifts in the Fe−His stretching frequency and correlate them to the local electrostatic environment directly above the heme iron. The position of band III is also seen to be affected by perturbations in the distal heme environment and may be influenced by other factors in addition to the displacement of the iron from the heme plane, e.g., the presence of histidine at E7. The similarity in the position of band III for WT and the Leu29Phe mutant (with and without distal pocket water, respectively) suggests that the role of water in shifting the position of band III in the absorption spectrum is minimal.

The magnitude of the shift in the Fe−His frequency produced by perturbing the distal pocket environment in SW deoxyMb is considerably smaller than that associated with the allosteric conformations in hemoglobin, and there is no direct and simple correlation between changes in the Fe−His frequency and the position of band III. Therefore, when these spectroscopic markers are used as structural probes of the heme active site, care must be taken to consider the role of "distal pocket effects", such as hydration or polarity, before drawing firm conclusions concerning changes in the proximal linkage.

ACKNOWLEDGMENT

We thank John Olson for graciously sending us a sample of the Leu29Phe mutant and a "fresh" sample of the His64Gly mutant. We also thank Wei Wang for valuable discussions, and Yu-Hui Chiu for assisting with the data analysis.

REFERENCES

Abe, M., Kitagawa, T., & Kyogoku, Y. (1978) *J. Chem. Phys. 69*, 4526.

Argade, P. V., Sassaroli, M., Rousseau, D. L., Inubushi, T., Ikeda-Saito, M., & Lapidot, A. (1984) *J. Am. Chem. Soc. 106*, 6593.

Campbell, B. F., Chance, M. R., & Friedman, J. M. (1987) *Science 238*, 373.

Carver, T. E., Brantley, R. E., Jr., Singleton, E. W., Arduini, R. M., Quillin, M. L., Phillips, G. N., Jr., & Olson, J. S. (1992) *J. Biol. Chem. 267*, 14443.

Chavez, M. D., Courtney, H., Chance, M. R., Kiula, D., Nocek, J., Hoffman, B. M., Friedman, J. M., & Ondrias, M. R. (1990) *Biochemistry 29*, 4844.

Cordone, L., Cupane, A., Leone, M., & Vitrano, E. (1990) *Biopolymers 29*, 639.

Cupane, A., Leone, M., Vitrano, E., & Cordone, L. (1988) *Biopolymers 27*, 1977.

Eaton, W. A., Hanson, L. K., Stephens, P. J., Sutherland, J. C., & Dunn, J. B. R. (1978) *J. Am. Chem. Soc. 100*, 4991.

Egeberg, K. D., Springer, B. A., Martinis, S. A., Sligar, S. G., Morikis, D., & Champion, P. M. (1990) *Biochemistry 29*, 9783.

Fiamingo, F. G., & Alben, J. O. (1985) *Biochemistry 24*, 7964.

Gilch, H., Dreybrodt, W., & Schweitzer-Stenner, R. (1995) *Biophys. J. 69*, 214.

Gilles-Gonzalez, M.-A., Gonzalez, G., Perutz, M. F., Kiger, L., Marden, M. C., & Poyart, C. (1994) *Biochemistry 33*, 8067.

Hargrove, M. S., Singleton, E. W., Quillin, M. L., Ortiz, L. A., Phillips, G. N., Jr., Mathews, A. J., & Olson, J. S. (1994) *J. Biol. Chem. 269*, 4207.

Hu, S., Smith, K. M., & Spiro, T. G. (1996) *J. Am. Chem. Soc. 118*, 12638.

Iizuka, T., Yamamoto, H., Kotani, M., & Yonetani, T. (1974) *Biochim. Biophys. Acta 371*, 126.

Ikeda-Saito, M., Hori, H., Andersson, L. A., Prince, R. C., Pickering, I. J., George, G. N., Sanders, C. R., II, Lutz, R. S., McKelvey, E. J., & Mattera, R. (1992) *J. Biol. Chem. 267*, 22843.

Jackson, T. A., Lim, M., & Anfinrud, P. A. (1994) *Chem. Phys. 180*, 131.

Kiger, L., Stetzkowski-Marden, F., Poyart, C., & Marden, M. C. (1995) *Eur. J. Biochem. 228*, 665.

Kitagawa, T., Nagai, K., & Tsubaki, M. (1979) *FEBS Lett. 104*, 376.

La Mar, G. N., Dalichow, F., Zhao, X., Dou, Y., Ikeda-Saito, M., Chiu, M. L., & Sligar, S. (1994) *J. Biol. Chem. 269*, 29629.

Li, X.-Y., Czernuszewicz, R. S., Kincaid, J. R., Su, Y. O., & Spiro, T. G. (1990) *J. Phys. Chem. 94*, 31.

Matsukawa, S., Mawatari, K., Yoneyama, Y., & Kitagawa, T. (1985) *J. Am. Chem. Soc. 107*, 1108.

Morikis, D. (1990) Ph.D. Thesis, Northeastern University, Boston, MA.

Morikis, D., Champion, P. M., Springer, B. A., & Sligar, S. G. (1989) *Biochemistry 28*, 4791.

Morikis, D., Champion, P. M., Springer, B. A., Egeberg, K., & Sligar, S. G. (1990) *J. Biol. Chem. 265*, 12143.

Nagai, K., & Kitagawa, T. (1980) *Proc. Natl. Acad. Sci. U.S.A. 77*, 2033.

Nienhaus, G. U., Mourant, J. R., & Frauenfelder, H. (1992) *Proc. Natl. Acad. Sci. U.S.A. 89*, 2902.

Palaniappan, V., & Bocian, D. F. (1994) *Biochemistry 33*, 14264.

Pin, S., Alpert, B., Cortès, R., Ascoe, I., Chiu, M. L., & Sligar, S. (1994) *Biochemistry 33*, 11618.

Quillin, M. L. (1995) Ph.D. Thesis, Rice University, Houston, TX.

Quillin, M. L., Arduini, R. M., Olson, J. S., & Phillips, G. N., Jr. (1993) *J. Mol. Biol. 234*, 140.

Rousseau, D. L., & Friedman, J. M. (1988) in *Biological Applications of Raman Spectroscopy* (Spiro, T. G., Ed.) Vol. 3, pp 172−180, John Wiley & Sons, New York.

Sage, J. T., & Champion, P. M. (1996) in *Comprehensive Supramolecular Chemistry* (Suslick, K. S., Ed.) Vol. 5, pp 171−218, Pergamon, Oxford, U. K.

Sage, J. T., Schomacker, K. T., & Champion, P. M. (1995) *J. Phys. Chem. 99*, 3394.

Sassaroli, M., & Rousseau, D. L. (1987) *Biochemistry 26*, 3092.

Schlichting, I., Berendzen, J., Phillips, G. N., Jr., & Sweet, R. M. (1994) *Nature 371*, 808.

Schulte, A., Buchter, S., Galkin, O., & Williams, C. (1995) *J. Am. Chem. Soc. 117*, 10149.

Springer, B. A., & Sligar, S. G. (1987) *Proc. Natl. Acad. Sci. U.S.A. 84*, 8961.

Springer, B. A., Egeberg, K. D., Sligar, S. G., Rohlfs, R. J., Mathews, A. J., & Olson, J. S. (1989) *J. Biol. Chem. 264*, 3057.

Springer, B. A., Sligar, S. G., Olson, J. S., & Phillips, G. N., Jr. (1994) *Chem. Rev. 94*, 699.

Šrajer, V., & Champion, P. M. (1991) *Biochemistry 30*, 7390.

Steinbach, P. L., Ansari, A., Berendzen, J., Braunstein, D., Chu, K., Cowen, B. R., Ehrenstein, D., Frauenfelder, H., Johnson, B., Lamb, D. C., Luck, S., Mourant, J. R., Neinhaus, G. U., Ormos, P., Phillipp, R., Xie, A., & Young, R. D. (1991) *Biochemistry 30*, 3988.

Varadarajan, R., Lambright, D. G., & Boxer, S. G. (1989) *Biochemistry 28*, 3771.

Teng, T.-Y. Šrajer, V., & Moffat, K. (1994) *Struc. Biol. 1*, 701.

Wells, A. V., Sage, J. T., Morikis, D., Champion, P. M., Chiu, M. L., & Sligar, S. G. (1991) *J. Am. Chem. Soc. 113*, 9655.

BI9710075